

Synthesis and Temperature sensitivity of Er^{3+} green upconverted Luminescence in yttrium oxysulfate phosphor

J.Rawat¹, S.Ray²

^{1,2}Department of Physical Science, Rabindranath Tagore University

Email: vyotirawatresearch@gmail.com

Abstract: *Infrared-to-green upconverted emissions of Er^{3+} -doped $\text{Y}_2\text{O}_2\text{SO}_4$ yttrium oxysulfate phosphor have been studied in order to develop an optical temperature sensor both in the biological range, from 296 up to 330 K, as well as in the industrial application range up to 475 K. Strong green, red, and near-infrared energy transfer-induced upconverted emission were observed when exciting the sample at 980 nm. In particular, the green thermalized bands show a relative sensitivity with temperature of $1.1\% \text{K}^{-1}$ at 296 K, among the highest found in literature. This result suggests that the Er^{3+} -doped yttrium oxysulfate can be used as an optical temperature sensor by exciting in the infrared range for biomedicine and industrial applications.*

Keywords: *Oxysulfate phosphor, Optical temperature sensor, Converted emission, Green thermalized, Doped yttrium oxysulfate.*

1. INTRODUCTION

Luminescence thermometry exploits the relationship between temperature and luminescence properties to achieve thermal sensing from the spatial and spectral analysis of the light generated from the object to be thermally imaged [1]. It is based on temperature induced changes in the spectroscopic (luminescence intensity or energy shifts, or lifetime or polarization changes) properties of the optically active ion in a given material (glass, glass-ceramic, crystal or nanocrystal) [1,2]. The determination of temperature by taking advantage of the thermal sensitivity of the optical properties of materials have been shown in organic fluorophores, metal complexes, quantum and carbon dots, gold nanorods and rare-earth doped glasses, crystals and nanocrystals [1-4]. In particular, rare-earth (RE^{3+}) doped materials have been extensively investigated for their wide optical applications in optomechanics [5], electronics [6], laser materials [7-9], bio-imaging, and in sensing applications, as pressure and temperature sensors.

The most used sensing technique is based on the temperature-dependent luminescence intensity ratio of RE^{3+} thermally coupled emissions [1-4], and their excitation via upconversion processes have attracted considerable interest in the last years. Upconversion is a non-linear process in which high energy visible and UV radiation is emitted by the rare earth ion after absorbing low energy near-infrared (NIR) laser radiation. Trivalent Erbium (Er^{3+}) ion is famous for its upconversion properties due to its ladder like energy levels, and Er^{3+} doped phosphor with intense green emission from thermally coupled levels $^4\text{S}_{3/2} - ^2\text{H}_{11/2}$ of Er^{3+} ($\Delta E \sim 800 \text{ cm}^{-1}$) have been considered as one of the most promising candidates for

luminescence thermometers. However, many times the RE^{3+} ion has been combined with Yb^{3+} one, such as $Y_2O_3:Yb^{3+}/Ho^{3+}$ and Yb^{3+}/Tm^{3+} or $NaLuF_4:Yb^{3+}/Gd^{3+}/Tm^{3+}$, to take advantage of the energy transfer-induced upconversion processes in optical temperature sensing.

2. MATERIALS AND METHOD

In order to prepare $(Y_{0.99}Er_{0.01})_2O_2SO_4$ optically active phosphor, the oxidation of oxysulfide precursor was obtained from yttrium oxide [Sigma Aldrich, 99.9%], erbium oxide [Sigma Aldrich, 99.9%], and carbon disulfide [Sigma Aldrich, $\geq 99.9\%$] using a high-energy planetary ball milling (Fritsch “pulverisette 6”), as described by Shoji and Sakurai. The precursor obtained was heated at 850 °C (1123 K) for 2 h and then cooled down to room temperature (RT).

The X-ray diffraction (XRD) pattern of $Y_2O_2SO_4:Er^{3+}$ (1 mol%) was obtained on a conventional diffractometer (PANalytical X'Pert PRO) equipped with a primary monochromator using the $Cu K_{\alpha 1}$ radiation as shown in Fig. 1). It has been identified by an accurate pattern matching with the ICDD data (file number 00-053-0168), having a monoclinic symmetry with the space group $C2/c$ and with lattice parameters $a=13.3072 \text{ \AA}$, $b=4.1465 \text{ \AA}$, $c=8.0205 \text{ \AA}$, $\beta=107.64^\circ$, and $Z=4$. The low concentration of Er^{3+} ions had no significant influence on these parameters, and also a negligible residual Y_2O_3 phase has been found.

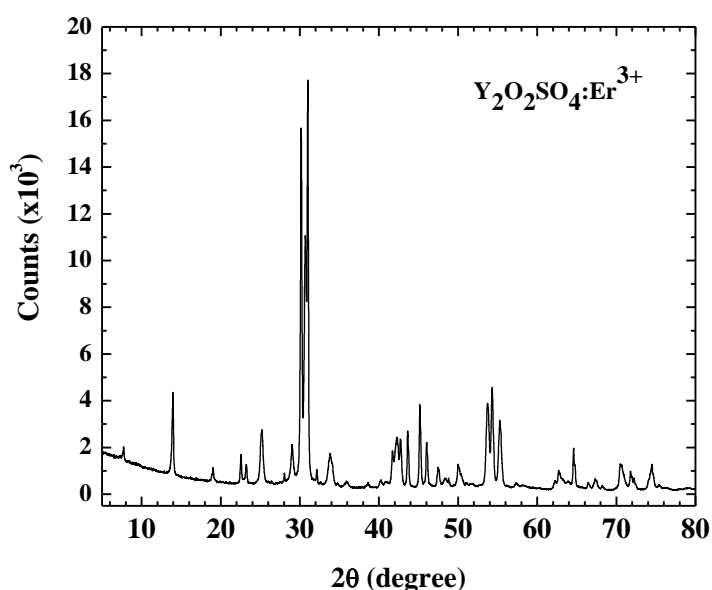


Fig. 4.1 X-ray diffraction pattern of the $Y_2O_2SO_4:Er^{3+}$ phosphor

Temperature-dependent upconverted luminescence experiments from RT up to 473 K were carried out in a tubular electric furnace where the sample was placed at its center and heated at a rate of 1 K/min, while temperature was controlled with a type K thermocouple connected to a voltmeter (Fluke Calibrator 714). The 975 nm laser radiation of a tunable cwTi: sapphire

laser (Spectra Physics 3900S) pumped by a 532 nm diode laser (Spectra Physics Millennia Prime Laser 15SJSPG) was used to excite the Er^{3+} ions from one side of the furnace. The power of the laser was kept low enough to avoid heating the sample. The upconverted green emissions were collimated by a lens located on the other exit side, and then focalized with another lens into an optical fiber coupled to a 0.3 m focal length, single grating spectrometer (Andor Shamrock 303i) equipped with a Peltier cooled silicon CCD camera (Andor Newton DU490A-1.7), with a resolution of 0.7 nm ($\sim 25 \text{ cm}^{-1}$) and an integration time of 4 s. Luminescence dynamics experiments were carried out by exciting the sample with a pulsed parametric oscillator OPO (EKSPLA/NT342/3/UVE) using an oscilloscope (LeCroy WS424) coupled to the detection system (Hamamatsu R-928) with an impedance of 50 Ω , providing a temporal resolution of 20 ns. All spectra were corrected for the spectral response of the equipment.

Luminescence intensity ratio (LIR) technique

In this work, the luminescence (or fluorescence) intensity ratio (LIR) technique has been applied to the green upconverted emissions of Er^{3+} doped in $\text{Y}_2\text{O}_3\text{SO}_4$ matrix in order to obtain a temperature scale. In this technique, the emission intensities of two levels which are very close to each other in energy, i.e. ${}^2\text{H}_{11/2}$ and ${}^4\text{S}_{3/2}$; thermalized levels of Er^{3+} , are recorded as a function of temperature and interpreted in terms of a simple three-level scheme system, taking into account the spontaneous emission probabilities of the ground state E_1 , and the two thermalized levels E_2 and E_3 as presented in Fig. 2. The (average) energy gap between these thermalized levels, $\Delta E = E_3 - E_2$, is small enough to allow a thermally-induced population redistribution of both multiplets that, in a thermal “quasi-equilibrium”, would follow the Boltzmann’s distribution. The ratio of these intensities does not (appreciably) depend on the laser source, if its power is kept low enough, but only depend on the population proportionality of the involved levels and their probabilities. Hence, the relationship between the relative populations of the thermalized levels R , and the temperature follows the Boltzmann’s distribution law, which can be described by the following equation [1-4]

$$R = \frac{I_{31}}{I_{21}} = \frac{c_{31}(\nu)}{c_{21}(\nu)} \cdot \frac{A_{31}g_3hv_{31}}{A_{21}g_2hv_{21}} \cdot e^{-\Delta E/k_B T} = C \cdot e^{-\Delta E/k_B T} \quad (1)$$

Where I_{31} , I_{21} are the integrated emission intensities (area under the emission bands) of the ${}^2\text{H}_{11/2}$ and ${}^4\text{S}_{3/2}$ thermalized levels, respectively; A_{31} and A_{21} are the spontaneous radiative emission rates of the E_3 and E_2 levels to the E_1 level, respectively as displayed in Fig. 2, which can only be estimated using the Judd-Ofelt Theory; g_2 , g_3 are the $(2J+1)$ degeneracies of each ${}^{2S+1}L_J$ multiplet; ΔE is the energy gap between the pair of thermalized levels in cm^{-1} and taking the barycenter of each multiplet; k_B is the Boltzmann constant; T is temperature in K; and $c_{ij}(\nu)$ is related to the energy (wavelength) dependence of the instrument response in the spectral range of each emission, which in this case can be considered equals to the unity since the thermalized emission spectra have been corrected from it.

The absolute sensitivity gives, in this case, a measure of the rate of change of the luminescence with temperature, which strongly depends on the pre-exponential factor of Eq. (1),

$$S_A = \left| \frac{dR}{dT} \right| = \frac{E_{32}}{k_B T^2} R \quad (2)$$

It is worth noting that the addition of the (c_{31}/c_{21}) ratio in Eqs. (1) and (2) makes the emission spectra totally independent of the experimental setup, and allows comparing the luminescence intensity ratio R and the absolute sensitivity S_A of different materials (glasses, glass-ceramics, crystals or nanocrystals) that uses the Er^{3+} ions as optical temperature sensor.

3. RESULTS AND DISCUSSION

Stokes and up converted emissions

Green, red, and near-infrared (NIR) Stokes emissions can be observed after a resonant excitation of the $^4\text{F}_{7/2}$ multiplet with a 488 nm laser light as presented in Fig. 2. After the absorption, there are different non-radiative multiphonon and energy transfer processes from the $^4\text{F}_{7/2}$ multiplet that populates the $^4\text{S}_{3/2}$ and $^4\text{F}_{9/2}$ emitting levels. In addition, and due to thermalization processes, the energy close to $^2\text{H}_{11/2}$ multiplet is also populated at the expenses of the population of the $^4\text{S}_{3/2}$ doublet multiplet. Thus, strong green emissions associated with the $(^2\text{H}_{11/2}, ^4\text{S}_{3/2}) \rightarrow ^4\text{I}_{15/2}$ transitions can be compared with the less intense red $^4\text{F}_{9/2} \rightarrow ^4\text{I}_{15/2}$ and NIR $(^2\text{H}_{11/2}, ^4\text{S}_{3/2}) \rightarrow ^4\text{I}_{13/2}$ ones as shown in Fig. 2. It is worthwhile to mention that the hypersensitivity of the absorption and emission probabilities of the $^2\text{H}_{11/2} \rightarrow ^4\text{I}_{15/2}$ transition to the distortion of the $\text{Er}^{3+}\text{-O}^{2-}$ local environment with respect to a pure inversion symmetry site. According to the Judd-Ofelt theory, this sensitivity can be quantified by a relatively large value of the Ω_2 parameter. On the other side, the structure of peaks of each emission band, associated with electronic transitions between Stark levels of the multiplets, reflexes the incorporation of the Er^{3+} ions at the C_{2v} crystalline site substituting the Y^{3+} ion, which show similar ionic radius, with the subsequent complete breakdown of the degeneracy of the $2\text{S}+1\text{L}_J$ multiplets.

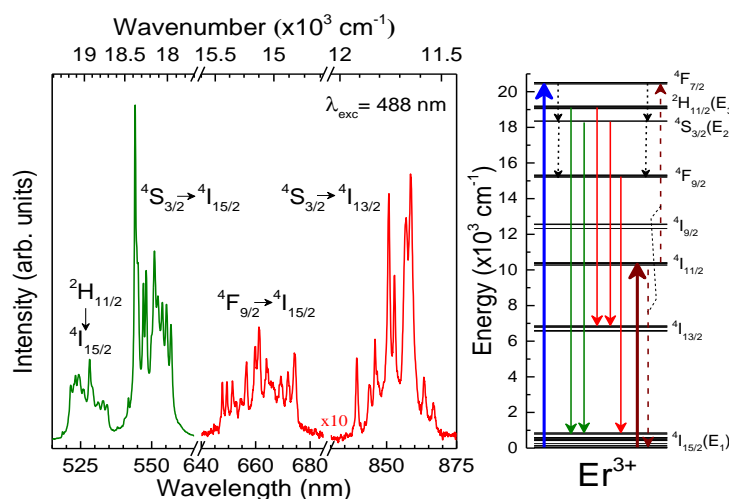


Fig. 4.2 (Left) Stokes luminescence spectrum of Er^{3+} in $\text{Y}_2\text{O}_2\text{SO}_4$ phosphor obtained at room temperature exciting resonantly the $^4\text{I}_{15/2} \rightarrow ^4\text{F}_{7/2}$ absorption band under 488 nm laser excitation. (Right) Partial energy level diagram of Er^{3+} in $\text{Y}_2\text{O}_2\text{SO}_4$ structure. Absorption at 488 nm (blue arrow) and 980 nm (red-brown arrow), emission (green and red arrows), multiphonon de-excitation (dotted arrows) and energy transfer (dashed red-brown arrows) selected processes are also shown.

NIR-to-visible and NIR-to-NIR upconverted (UC) emissions can be also observed, the strong green emission by the naked eyes, when exciting resonantly either the $^4\text{I}_{9/2}$ multiplet with a 800 nm laser light or the $^4\text{I}_{11/2}$ multiplet with a 975 nm radiation. Upconversion is a non-linear,

two-step process in which the optically active ion is first excited to an intermediate level and, in a second step, promoted to the high energy emitting levels as displayed in energy level diagram in Fig. 2. In this study, we will focus our attention on the $(^2H_{11/2}, ^4S_{3/2}) \rightarrow ^4I_{15/2}$ green UC emissions in $Y_2O_2SO_4$ powder doped with 1.0 mol% of Er^{3+} ions under 975 nm laser excitation as presented in Fig. 3, which completely resemble those Stokes emissions as shown in Fig. 2. These green UC emissions will be later calibrated for optical temperature sensing, since they combine high intensities and high quantum efficiencies with a large hypersensitivity of the transition of the upper thermalized $^2H_{11/2}$ level (level E_3 in Fig. 2) to the ground state (level E_1).

The non-linearity of the UC processes can be easily confirmed by analyzing the dependence of the UC emissions with the 975 nm laser pump power. Since it is a non-linear process, the number of photons N , or their equivalence in quanta energy, that is involved in the population of the emitting levels can be obtained from the following formula: $I_{UC} \propto (I_{PUMP})^N$, where I_{UC} is the intensity of the UC emission, i.e. area under

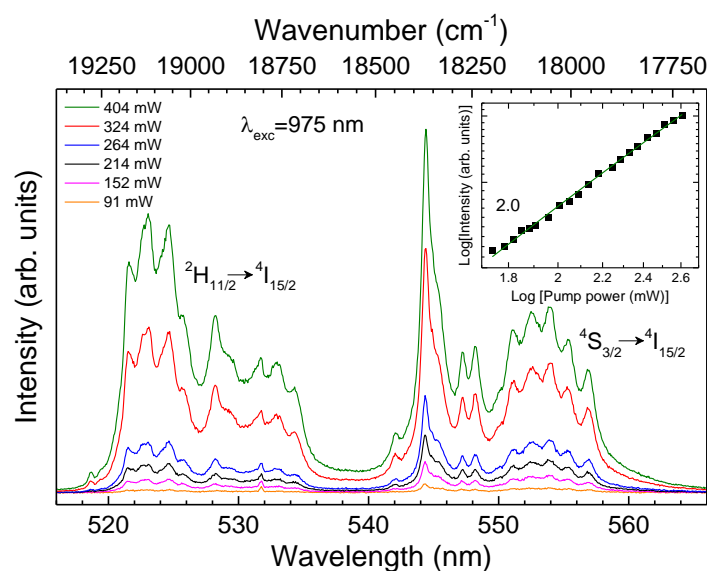


Fig. 4.3 Upconverted emission spectra of $Y_2O_2SO_4: Er^{3+}$ 1.0 mol% phosphor under different pump powers of the 975 nm laser at room temperature. Inset shows the upconverted intensities of $Y_2O_2SO_4: Er^{3+}$ 1.0 mol% phosphor as a function of the pump power at 975 nm in a double-log scale.

4. CONCLUSIONS

Energy transfer-induced upconverted green thermalized luminescence of Er^{3+} in $Y_2O_2SO_4$ yttrium oxysulfate phosphor has been calibrated as an optical temperature sensor both in the biological range, from 296 up to 330 K, as well as in the industrial application range up to 475 K when exciting the sample at 980 nm. The green thermalized bands show a relative sensitivity with temperature of $1.1 \% K^{-1}$ at 296 K, among the highest found in literature. $Y_2O_2SO_4: Er^{3+}$ (1.0 mol%) phosphor shows relatively high absolute and relative sensitivities, and it can be considered as a potential candidate to become an optical temperature sensor based on the LIR technique working in the VIS range exciting in NIR, for both temperature ranges, those with applications in biological and biomedicine as well as in higher temperature industrial applications.

5. REFERENCES

- [1] L.D. Brites, C. D. S. Millan, and L. Carlos, “Lanthanides in luminescent thermometry”, in: Handbook on the Physics and Chemistry of Rare Earths Incl. Actinides, J.V.G. Bünzli, V.K. Pecharsky (Eds.), Elsevier B.V., Amsterdam, 2016: pp. 339-427. DOI:10.1016/B978-0-12-800202-5.16001-1.
- [2] D. Jaque, and F. Vetrone, “Luminescence nanothermometry”, *Nanoscale* 4 (2012) 4301-4326. DOI: 10.1039/C2NR30764B.
- [3] C.D.S. Brites, P.P. Lima, N.J.O. Silva, A. Millán, V.S. Amaral, F. Palacio, and L.D. Carlos, “Thermometry at the nanoscale”, *Nanoscale* 4 (2012) 4799–4829. DOI:10.1039/c2nr30663h
- [4] L.D. Carlos, F. Palacio, eds., “Thermometry at the Nanoscale”, Royal Society of Chemistry, Cambridge, 2015. DOI:10.1039/9781782622031.
- [5] D. Navarro-Urrios, M. Baselga, F. Ferrarese Lupi, L.L. Martín, C. Pérez-Rodríguez, V. Lavín, I.R. Martín, B. Garrido, and N.E. Capuj, “Local characterization of rare-earth-doped single microspheres by combined microtransmission and microphotoluminescence techniques”, *J. Opt. Soc. Am. B* 29 (2012) 3293-3298. DOI:10.1364/JOSAB.29.003293
- [6] F. Zhang, G.B. Braun, Y. Shi, Y. Zhang, X. Sun, N.O. Reich, D. Zhao, G. Stucky, J. Hao, L.H. Fischer, G.S. Harms, O.S. Wolfbeis, Z.L. Wang, J. Hao, H.L.W. Chan, W.T. Wong, and K.L. Wong, “Metal-ion doped luminescent thin films for optoelectronic applications”, *J. Mater. Chem. C* 8 (2013) 2850-2851. DOI:10.1002/sml.201102703.
- [7] J. J. Romero, E. Montoya, L.E. Bausá, F. Agulló-Rueda, M.R.B. Andreetta, and A. C. Hernandez, “Multi-wavelength laser action of Nd³⁺:YAlO₃ single crystals grown by the laser heated pedestal growth method”, *Opt. Mater.* 24 (2004) 643-650. DOI: 10.1016/S0925-3467(03)00179-4
- [8] Iparraguirre, J. Azkargorta, J.M. Fernández-Navarro, M. Al-Saleh, J. Fernández, and R. Balda, “Laser action and upconversion of Nd³⁺ in tellurite bulk glass”, *J. Non. Cryst. Solids.* 353 (2007) 990-992. DOI: 10.1016/j.jnoncrysol.2006.12.103
- [9] M.J. Weber, M. Bass, T.E. Varitimos, and D.P. Bua, “Laser action from Ho³⁺, Er³⁺, and Tm³⁺ in YAlO₃”, *IEEE J. Quantum Electron.* QE-9 (1973) 1079-1086. DOI:10.1109/JQE.1973.1077426.